Crystal defects and spin tunneling in single crystals of Mn_{12} clusters

J.M. Hernandez, F. Torres and J. Tejada
Dept. Fisica Fonamental, Univ. Barcelona. Diagonal 647. 08028 Barcelona. Spain

E. Molins
Institut de Ciència de Materials de Barcelona (CSIC). Campus UAB. 08193 Cerdanyola. Spain

(Received February 1, 2008)

Abstract

The question addressed in this paper is that of the influence of the density of dislocations on the spin tunneling in Mn_{12} clusters. We have determined the variation in the mosaicity of the crystal structure of fresh and thermally treated single crystals of Mn_{12} by analyzing the widening of low angle X-ray diffraction peaks. It has also been well established from both isothermal magnetization and relaxation experiments that there is a broad distribution of tunneling rates which is shifted to higher rates when increases the density of dislocations.

PACS: 75.45.+j, 75.50.Xx

Within the last few years molecular clusters have emerged as a truly interdisciplinary field. This is so because these materials allow to test the border between quantum and classical mechanics [1], they may be used as a hardware for quantum computers [2,3] and for low temperature magnetic cooling [4]. The magnetic hysteresis in molecular clusters results from the existence of $2S+1$ spin levels in the two wells of the magnetic anisotropy barrier. These spin levels correspond to the different projections of the total spin of each molecule on its easy axis. Mn_{12} molecular clusters have $S=10$ at low temperature and are equivalent to a single domain particle with constant modulus of its magnetic moment, $20\mu_B$, the orientation of which depends on the ratio between the temperature and the barrier height existing between the up and down orientations. The occurrence of magnetic relaxation at temperatures at which the thermal fluctuations die out is due to spin resonant tunneling between degenerate S_Z states in the two wells of the anisotropy potential wells [5–15]. To the first approximation the spin Hamiltonian used previously [5–15] to fit the magnetic data obtained for the different Mn_{12} molecular clusters is written as

$$\mathcal{H} = -DS_Z^2 + \mathcal{H}' + \mathcal{H}_{dip} + \mathcal{H}_{hf} \tag{0.1}$$

where $D = 0.65$ K [16–18] and $\mathcal{H}'$ contains anisotropy terms of fourth order of the spin operator [16–19] which depend on the symmetry of the crystal. The two last terms correspond

to the contribution of both dipolar and hyperfine fields to the transverse magnetic field. The first term of equation 0.1 generates spin levels S_Z inside each well while the symmetry violating terms inducing tunneling are those associated with the transverse component of the magnetic anisotropy and the transverse dipolar and hyperfine fields. Very recently, however, Chudnovsky and Garanin [20] have suggested that tunneling due to the magnetoelastic coupling, $\mathcal{H}_{me}$, may be even larger that those due to the terms written in equation 0.1. This may be so as a consequence of the local transverse anisotropy and magnetic fields associated to dislocations. Here we present experimental evidence on the effect of defects, mostly dislocations, on both the rate of spin tunneling and the law of relaxation in two Mn_{12} single crystals.

The Mn_{12}Ac forms a molecular crystal of tetragonal symmetry with the lattice parameters $a = 1.732$ nm and $c = 1.239$ nm [21]. The unit cell contains two $Mn_{12}O_{12}$ molecules surrounded by four water molecules and two acetic acid molecules. The Mn_{12} 2Cl-benzoate, Mn_{12}Cl, forms a molecular crystal of orthorhombic structure with the lattice parameters $a = 2.275$ nm, $b = 1.803$ nm and $c = 1.732$ nm with two molecules per unit cell [22,23]. The magnetic core and the local symmetry of each molecule are identical to the case of $Mn_1$2Ac with the only difference that the easy axes of Mn_{12}Cl lie alternatively on the direction (011) or $(0\overline{1}1)$, being nearly perpendicular to their nearest neighbors. Fresh single crystals of Mn_{12}Ac and Mn_{12}Cl were first characterized by X-ray diffraction techniques and then we carried out the magnetic studies. The next step was to cycle the temperature of the single crystals between 80 K and 300 K by introducing them in liquid nitrogen during five minutes and in water for also five minutes. This thermal cycle was repeated four times. Then we performed new X-ray diffraction and magnetic characterization. A second heat treatment, similar to the first one, followed by both X-ray and magnetic characterization was also performed. During all these operations the single crystals were kept glued on the top of a glass capilar.

The thermal treatment suppose a rapid change in the temperature of the surrounding air of the crystal of about 200 K. When the crystal core is still at the initial temperature, the surface of the crystal starts to cool down. This large temperature gradient generates radial and tangential tensions that favor the propagation of dislocations across the crystal, probably starting at point defects frozen during the growing of the crystal and during the X-ray irradiation (it should be taken into account that for the X-ray characterization the crystals were irradiated during 24 hours). The extension of these dislocations by the whole crystal converts an initial single crystal in a multidomain crystal which each element is slightly misaligned in front of its neighbors. This is what is known as a mosaic crystal and the amount of misalignment is related to the widening of the diffraction peaks. The peak widening observed in our experiments is of some tenths of a degree. Due to this low value, the crystals after the heat treatments are still considered as a single crystals but with a larger mosaicity.

To better determine the variation in the mosaicity with the heat treatment [24–26], we have focused our attention on low angle reflection peaks in order to minimize the widening associated to the lack of monochromaticity ($MoK_{\alpha 1}$ and $MoK_{\alpha 2}$). After checking the crystal parameters and getting the crystal orientation by using a four-circle single-crystal X-ray diffractometer, we choose the reflections (± 2 ± 2 ± 2) for the comparison before and after the heat treatment as they were low angle and intense. In Figure 1 we show the $\omega - \theta$

plot of the ($\overline{2}22$) reflection, for the Mn_{12}Cl single crystal, before (left), after the first heat treatment (center) and after the second heat treatment (right). The insert clearly shows the enlargement of the reflection peak along ω due to the increase of the mosaicity while keeping constant the 2θ-width. In the final state the flattening in ω even overcomes the scan width. Assuming that the average distance between dislocations is inversely related to the ω-widening and taking into account that such ω widening approximately doubles after each thermal treatment, see Figure 1, it may be conclude that the number of dislocation increases near an order of magnitude after the heat treatment. Similar results were observed in the low angle diffraction peaks for the Mn_{12}Ac single crystal.

The performed magnetic characterization of the single crystals before and after the heat treatment, include hysteresis cycles at different temperatures and relaxation experiments over the resonance at zero field by changing the sweeping rate of the magnetic field . The first experimental evidence that something is going on with the heat treatment, came out from the magnetic relaxation data at zero field, see Figure 2. In these measurements the single crystals were first placed in a field $H = 30$ kOe at $T = 10$ K, then they were cooled until the desired temperature and the field was then switched off. The data displayed in Figure 2 and those obtained at T =2.0 and 2.2 K for the two single crystals show that both the amount of magnetization relaxing per unit time and the relaxation rate are larger after the heat treatments. To see better this effect, we show in figure 2B the calculation of the relaxation rate, Γ, at each time, which was deduced from the relaxing data by using the differential exponential law ($\Delta M = -M\Gamma\Delta t$). All these relaxation curves are, however, pretty well fitted, in the entire time interval, by stretched exponential functions, $M(t) = M_0 \exp(-a{\cdot}t^b)$ being both a and b depending on the concentration of dislocations.

In Figure 3 we show the field dependence of the differential susceptibility $\partial M/\partial H$ deduced from the hysteresis measurements recorded at two different temperatures for the Mn_{12}Cl single crystal before and after the second heat treatment. The position of the resonant peaks, where dM/dH is maximum, does not change with the heat treatment, indicating that the internal structure of the Mn_{12} clusters as well as the spin levels are not influenced by defects. The sweeping rate of the magnetic field in all these experiments was 10 Oe/s. In Table I we give the values of the area under each peak $\partial M/\partial H$ at the resonance fields at different temperatures. These data show that the intensity and width of the peak at zero field increase at all temperatures after the heat treatment. This corresponds to have a larger amount of magnetization tunneling at zero field at all temperatures. A similar enhancement is also detected for the tunneling processes contributing to the second, 5 kOe, and third resonance, 10 kOe, when the hysteresis is recorded at low temperature. The reduction in the intensity of the peaks at larger fields and higher temperature after the heat treatment with respect to those observed with the fresh material, corresponds to the fact that as we are studying the demagnetization process there is less magnetization to tunnel after crossing the zero field resonance. The temperature tends to reduce the differences in the observed $\partial M/\partial H$ peaks at high fields for the fresh and treated crystals as it should be due to the variation of the equilibrium magnetization with temperature and to the fact that the detected tunneling rates at large times do not change to much with the heat treatment. That is, there is always a fraction of molecules not affected by defects. These molecules show the same relaxation rate before and after the heat treatment.

Let us start the interpretation by commenting on the data shown in Figure 2B. These

data strongly support that the spin relaxation of our sample is a superposition of exponential decays with different rates

$$M(t) = M_0 \sum_i \exp(-\Gamma_i t) \tag{0.2}$$

Where M_0 is the initial magnetization, that is at t =0, and Γ_i should correspond to the relaxation rate for the different molecules affected or not by dislocations. The molecules near the core of the dislocations are those for which the magnetoelastic coupling is the largest and, consequently, show the strongest tunneling effect. That is, these are the molecules owing the largest tunneling rates. As we move away from the nucleus of the dislocations both the transverse anisotropy and transverse field become smaller and consequently decreases the spin tunneling rate for the molecules located far of dislocations, increasing therefore the number of molecules affected by dislocations and their tunneling rates. This is the reason why there is a distribution of relaxation times and the measured tunneling rates decreases as time is running. That is, the fresh single crystals and those thermally treated show a broad distribution of tunneling splittings, Δ. In fact, this is the reason why the relaxation rate of the magnetization for the fresh crystals show also a time-dependence. The gravity center of this distribution shifts to larger tunneling rates after the heat treatment as a consequence of having a larger density of dislocations. This interpretation is also supported by the results obtained from the hysteresis measurements. The crystals after the heat treatments have higher density of dislocations and show, at all temperatures, larger tunneling magnetization at the zero field resonance. The fact that the amount of magnetization relaxing at the resonance located at high fields decreases after the heat treatment reflects the fact that there is less magnetization to relax. We may, therefore, conclude that the variation in the crystal mosaicity detected in the X-ray experiments is fully correlated with the increase in the number of molecules relaxing faster which, as a matter of fact, are the molecules affected by dislocations.

We have also found that when sweeping the field through the zero field resonance, the relaxing magnetization normalized to its initial value, scales as a function of $T \ln(\nu\, r)$. This reflects the fact that in the presence of dislocations occur both, a broad distribution and the overlapping of the tunneling probability for the different spin levels.

Summarizing, we have shown and discussed magnetic data for two molecular single crystals which indicate that dislocations modify substantially the spin tunneling rate. The magnetic relaxation law is strongly affected by the existence of defects as a consequence of the overlapping of tunneling splittings for the different spin levels. The results are in agreement with a recent work on the nature of spin tunneling in Mn_{12}-Acetate [27] and in the broading of the EPR linewidths due to dislocations [28].

Acknowledgments.- The authors thank the EC Grant number IST-1999-29110 for financial support.

REFERENCES

[1] E.M. Chudnovsky, *Science* **274**, 938 (1996). P.C.E. Stamp, *Nature* **383**, 125 (1996). B. Schwarztchild, *Phys. Today* **50**, 17 (1997).

[2] M.N. Leuenberger and D. Loss, *Nature* **410**, 789 (2001).

[3] J. Tejada, E.M. Chudnovsky, E. del Barco, J.M. Hernandez and T.P. Spiller, *Nanotechnology* **12**, 181 (2001).

[4] F. Torres, J.M. Hernandez, X. Bohigas and J. Tejada, *Appl. Phys. Lett.* **77**, 3248 (2000).

[5] J.R. Friedman, M.P. Sarachik, J. Tejada and R. Ziolo, *Phys. Rev. Lett.* **76**, 3830 (1996).

[6] J.M. Hernandez, X.X. Zhang, F. Luis, J. Bartolomé, J. Tejada and R. Ziolo, *Europhys. Lett.* **35**, 301 (1996).

[7] L. Thomas, F. Lionti, R. Ballou, D. Gatteschi, R. Sessoli, B. Barbara, *Nature* **383**, 145 (1996).

[8] J.A.A.J. Perenboom, J.S. Brooks, S. Hill, T. Hathaway and N.S. Dalal, *Phys. Rev. B* **58**, 330 (1998).

[9] W. Wernsdorfer, R. Sessoli and D. Gatteschi, *Europhys. Lett.* **47**, 254 (1999)

[10] L. Bokacheva, A.D. Kent and M.A. Walters *Phys. Rev. Lett.* **85**, 403 (2000).

[11] D.A. Garanin and E.M. Chudnovsky, *Phys. Rev. B* **56**, 11102 (1997).

[12] F. Luis, J. Bartolomé and J.F. Fernández, *Phys. Rev. B* **57**, 505 (1998).

[13] N.V. Prokof'ev and P.C.E Stamp, *Phys. Rev. Lett.* **80**, 5794 (1998).

[14] M.N. Leuenberger and D. Loss, *Europhys. Lett.* **46**, 692 (1999).

[15] A. Garg, *Phys. Rev. Lett.* **81**, 1513 (1998)

[16] A.L. Barra *et al.*, *Phys. Rev. B* **56**, 8192 (1997).

[17] A.A. Mukin *et al.*, *Europhys. Lett.* **44**, 778 (1998).

[18] Y. Zhong *et al.*, *J. Appl. Phys.* **85**, 5636 (1999).

[19] I. Mirebeau *et al.*, *Phys. Rev. Lett.* **83**, 628 (1999).

[20] E.M.Chudnovsky and D.A.Garanin, *cond-mat/0105195*

[21] T. Lis *Acta Crystallogr.* **B36**, 2042 (1980).

[22] B. Albela, *PhD Thesis, Universitat Barcelona* (1996)

[23] F. Luis, J.M. Hernandez, J. Bartolomé and J. Tejada, *Nanotecnology* **10**, 86 (1999).

[24] R.I.Barabash, "X-ray Analysis of precipitation-related crystals with dislocation substructure". Pag 127-140 in " Defect and Microstructure analysis by diffraction" by R.L.Snyder, J.Fiala and H.J.Bunge. IUCr Monographs on Crystallography 10. Oxford University Press (1999).

[25] A.McL.Mathieson. *Acta Cryst.* **A38**, 378 (1982).

[26] A.McL. Mathieson and A.W. Stevenson. *Acta Cryst.* **A41**, 290 (1985); *ibid.* **A42**, 223 (1986).

[27] K.M. Mertes et. al., *cond-mat/0106579.*

[28] K. Park et. al. *cond-mat/0106276.*

TABLES

	Heat	**Resonance's area ($\times 10^{-4}$ emu)**			
T (K)	**treatment**	**0 kOe**	**5 kOe**	**10 kOe**	**15 kOe**
1.8	Before	19.6	< 1	10.0	54.6
	After 1st	25.5	< 1	14.1	54.7
	After 2nd	28.8	< 1	12.8	47.7
2.0	Before	17.3	5.2	33.6	46.5
	After 1st	20.6	7.9	44.1	40.4
	After 2nd	31.4	10.1	26.6	31.7
2.2	Before	22.1	15.5	60.9	24.4
	After 1st	33.5	24.0	52.6	23.3
	After 2nd	33.2	25.0	51.6	16.8
2.4	Before	22.5	44.6	43.8	4.1
	After 1st	33.6	44.1	28.3	3.2
	After 2nd	38.1	46.0	29.3	2.4

TABLE I. Areas below the differential susceptibility $\partial M/\partial H$ curves at the resonance peaks for the $Mn_{12}Cl$ single crystal before and after the first and second heat treatment deduced from hysteresis measurements recorded at different temperatures.

FIGURES

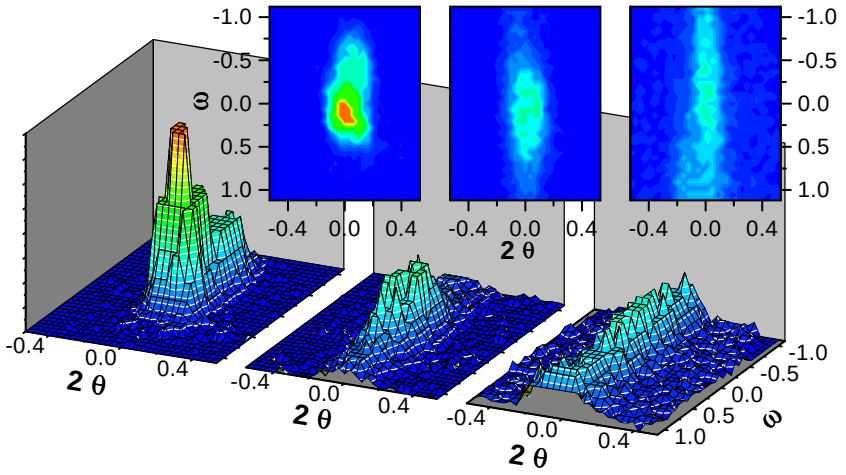

FIG. 1. $\omega - \theta$ plot of the $(\bar{2}22)$ reflection of the $Mn_{12}Cl$ crystal: before (left), after one heat treatment (center) and after two heat treatments (right) . The inserts clearly show the enlargement of the peak along ω due to the increase in mosaicity after the heat treatments, while keeping a constant θ-width. The flattening in ω even overcomes the scan width.

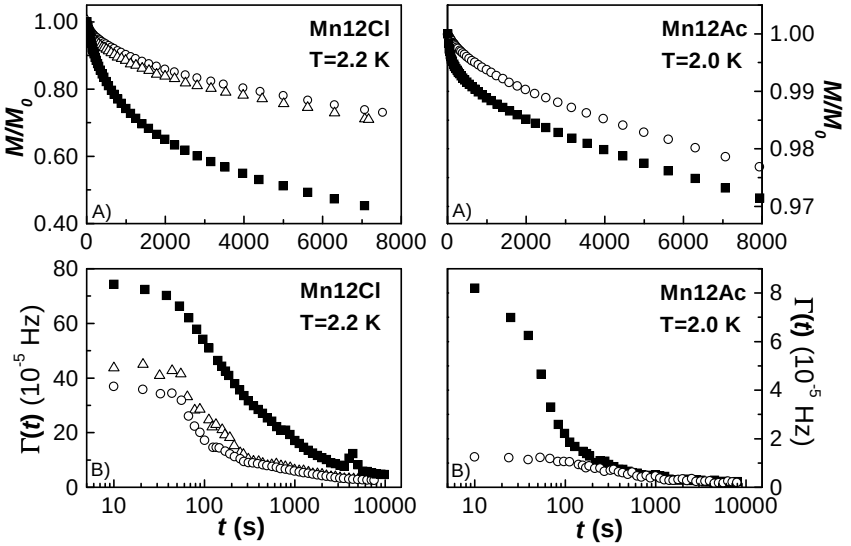

FIG. 2. A) Magnetic relaxation of single crystals of $Mn_{12}Ac$ and $Mn_{12}Cl$ at different temperatures before (open circles) and after (open triangles, solid squares) the heat treatments. B)Evolution with time of the effective relaxation rate corresponding to the data depicted on A. The relaxation rates at each time have been calculated as the time derivatives of the logarithm of the magnetization.

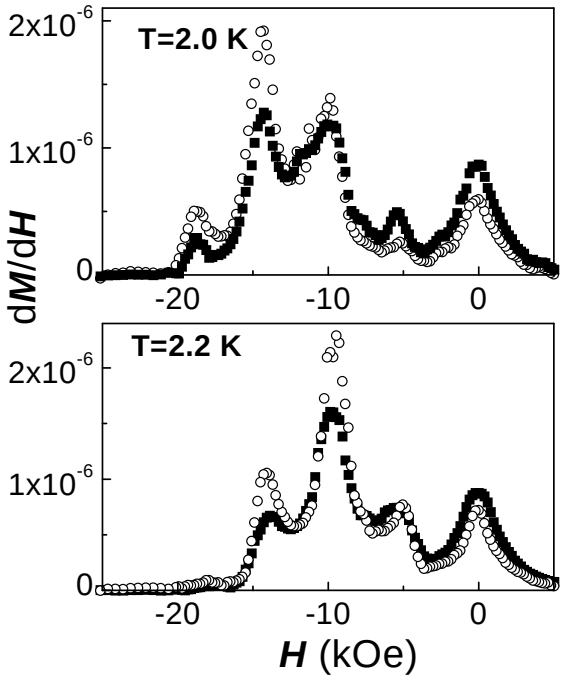

FIG. 3. Differential susceptibility, $\partial M/\partial H$, at the resonance fields deduced from the hysteresis cycles at different temperatures for the $Mn_{12}Cl$ single crystal, before (open circles) and after (solid squares) the heat treatments.